Real-Time Cooperative Control of a Distributed Illumination System Mid-term report

Tomás Martins-100102*
*Instituto Superior Técnico, Lisboa
Email: tomasmartins77@tecnico.ulisboa.pt

***Abstract*—This article addresses the problem of an illumination system using real using real-time control. This controller utilizes a LED and a LDR resistor that in conjuntion with an arduino Raspberry Pi Pico, can estimate the value of light in lux of an environment. The theoretical and real-world experiments provide substantial evidence regarding the effectiveness of this system, as indicated by the conclusive outcomes.**

***Index Terms*—PID controller, Arduino Raspberry Pi Pico, Anti-windup, bumpless transfer, Lux**

I. Introduction

The primary aim of this project is to develop a real-time, distributed illumination system. However, for the mid-term report, the focus is on constructing the controller system for one illumination unit. This involves creating a smart luminaire capable of adapting to user preferences. This will be achieved by utilizing an Arduino RPI Pico, an LDR resistor, and an LED. These components, integrated into a circuit inside a white enclosure, will simulate an office desk illumination system.

Given that the well-being of users is a central concern in illumination systems, our luminaire will employ a Proportional-Integral-Derivative (PID) controller. This controller is instrumental in ensuring smooth transitions between various light levels. It effectively manages changes in light intensity, whether initiated by user preferences or external environmental disturbances, such as variations in external lighting conditions.

The Arduino RPI Pico will serve as the brain of our system, orchestrating the interaction between the LDR resistor and LED. The Light Dependent Resistor (LDR) will act as the sensor, detecting changes in ambient light. The LED, controlled by the PID algorithm, will dynamically adjust its intensity to maintain optimal illumination based on user preferences.

To maintain a clean and controlled environment, all components will be housed within a white enclosure. This enclosure not only provides a visually uniform background but also contributes to the overall aesthetics of the system. It ensures that external factors do not interfere with the precision of the illumination adjustments, if not wanted.

Looking ahead, the successful implementation of this smart luminaire will serve as a foundation for the broader distributed illumination system. The insights gained from this initial phase will inform the expansion and integration of multiple units, culminating in a comprehensive and user-friendly lighting solution.

II. Methodology

A. Luminaire model

The luminaire model is assembled inside of a shoe box, in order to simulate the office space, the inside of the box must be white in order to have better reflective properties. The images shown in Figure 1 and 2 show the final illumination system, with the 3 luminaires stuck to the bottom of the box and the 3 CAN-BUS drivers outside to communicate between the different luminaires.

Fig. 1: External luminaire model

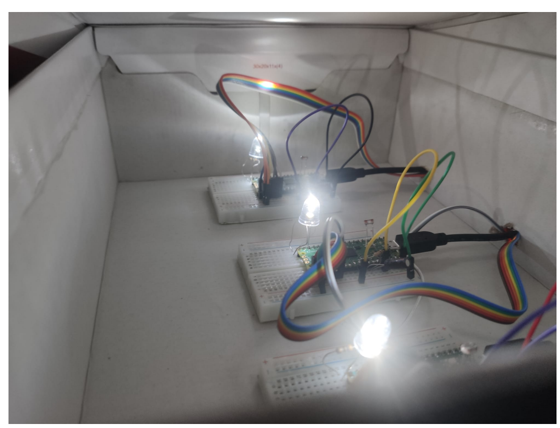

Fig. 2: Internal luminaire model

B. Illuminance measurement system

The illuminance measurement system is composed of three main components: the LED light emitter and the LDR receiver as seen in Figure 3 and then the conversion of the value received by the ADC from the LDR into lux.

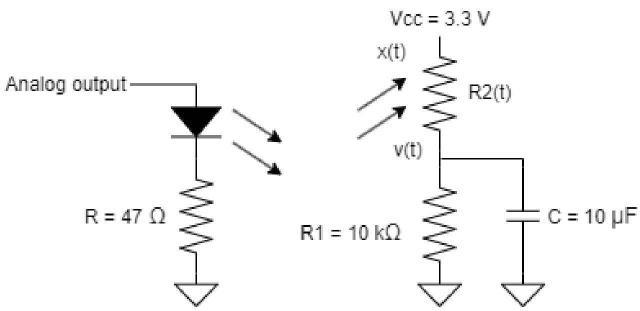

Fig. 3: LED driving and LDR reading circuits

There are some assumptions made in order to simplify the system, first of all, it is assumed that not only the LED driving circuit and LED response time are very fast, but also the light propagation in air.

$$x(t) = Gu(t) + o(t) \tag{1}$$

Considering the the system gain G ($\frac{Lux}{DutyCycle}$) and o the external illumination, it is easily deductible that if the the external illumination is subtracted this becomes a linear 0^{th} order system with static gain. $u(t)$ represents the LED command in duty cycle [0, 1].

Regarding the LDR sensor circuit, it is presumed that R_2(t) undergoes instantaneous changes. x(t) represents the value detected by the LDR, altering the voltage v(t) in the circuit. The Arduino reads this voltage within the range of 0 to 4095 as $v_{ADC}(t)$.

$$v(t) = \frac{v_{ADC}(t)}{ADCrange} V_{cc} \tag{2}$$

Where *ADCrange* = 4095 and V_{cc} = 3.3 V. The actual value of R_2 changes with the intensity of the light received, so in order to calculate it, we must know the equation of $R_2(t)$.

$$v(t) = \frac{R_1 R_2(t)}{R_1 + R_2(t)} V_{cc} \leftrightarrow R_2(t) = \frac{V_{cc} R_1}{v(t)} - R_1 \tag{3}$$

We can now compute $y(t)$ in LUX:

$$log_{10}(R_2(t)) = mlog_{10}(y(t)) + b \leftrightarrow y(t) = 10^{mlog(R_2(t))+b} \tag{4}$$

The parameter 'm' is derived from the LDR datasheet, and its specific value is -0.8 with a margin of error of ±0.1. This parameter characterizes the Light Dependent Resistor's behavior in response to varying light conditions.

On the other hand, 'b' is a value determined under specific conditions, precisely when the light intensity is 10 lux. At this illuminance level, the resistance of the photo resistor falls within the range of 150kΩ to 300kΩ. For the purpose of this project it is used the value 225kΩ, making *b*:

$$log_{10}(R_2) = mlog_{10}(LUX) + b \leftrightarrow b = log_{10}(225k\Omega) - m \tag{5}$$

C. Box gain

In order to understand how the light travels through the box, influencing the light received by the LDR, the overall system gain must be calculated every time the program starts, and is given by:

$$G = \frac{Lux_{max} - Lux_{min}}{1 - 0} \tag{6}$$

Where $Lux_{max/min}$ are the voltages read when the LED is at it's maximum or minimum value. The denominator is given by the duty cycle at these maximum and minimum values.

D. Controller

1) PID: The primary objective of implementing a controller in this project is to facilitate the swift adjustment of illuminance to a desired value (r) and to maintain it at the set-point in response to external disturbances, all while minimizing overshoots and oscillations for enhanced user comfort.

To achieve these goals, a Set-Point Weighting PID controller is employed, focusing solely on the proportional and integral parameters, as the derivative component proves to be less critical for our specific application.

The feedfoward expression is given by:

$$u_{ff}(t_k) = r(t_k) * b * K \tag{7}$$

Here, K and b is are set-point tuning variables. Also, $r(t_k)$ at each discrete time instant t_k, enters the controller as volts, in order to reduce non linear errors given by the conversion to lux.

The proportional term in discrete time is expressed as follows:

$$P(t_k) = -Ky(t_k) \tag{8}$$

This term contributes to the controller's ability to respond proportionally to the error between the desired set-point ($r(t_k)$) and the system's measured value ($y(t_k)$), both in volts.

The integral term is given by:

$$I(t_{k+1}) = I(t_k) + \frac{Kh}{Ti}(r(t_k) - y(t_k)) \tag{9}$$

In this equation, $r(t_k) - y(t_k)$ represents the error between the reference value and the measured value by the system.

To ensure effective control and responsiveness, a sampling time h of 10 milliseconds is employed in our system using a non-blocking *interrupt*. This leads to the computation of the control value ($u_{fb}(t_k)$) as the sum of the proportional and integral terms:

$$u_{fb}(t_k) = P(t_k) + I(t_k) \tag{10}$$

$$v(t_k) = u_{ff}(t_k) + u_{fb}(t_k) \tag{11}$$

E. Anti-windup

It is easily deducted that the integral term continues to grow if, for example the LED achieves it's maximum illuminance value, making it important to have some anti windup action, in this case with back-calculation. To implement this, values of $v(t_k)$ only operate in $u(t_k) \in [0,\ 1]$ and a change in the integral term is made:

$$I(t_{k+1}) = I(t_k)\frac{Kh}{Ti}(r(t_k)-y(t_k))+\frac{h}{Tt}(u(t_k)-v(t_k)) \quad (12)$$

This change, makes it that, if the controller saturates, the integral term will discharge faster when changing the value of T_t.

F. Bumpless transfer

If the user chooses to change the K and b constants when the system is running, the controller should have a smooth outcome of this change, this can be done with the following change in the integral term:

$$I(t_k)_{new} = I(t_k)_{old} + K_{old}(b_{old}e(t_k)) - K_{new}(b_{new}e(t_k)) \quad (13)$$

Where $e(t_k)$ is given by $r(t_k) - y(t_k)$. The final controller has the following block diagram:

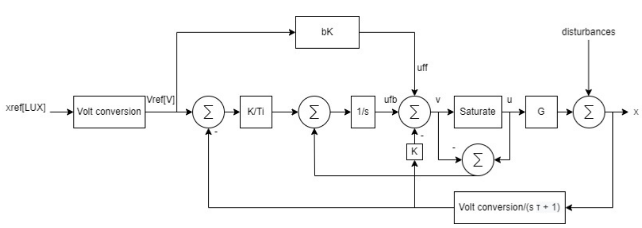

Fig. 4: Controller's block diagram

III. Parameters tuning

1) b parameter in lux conversion: In equation 5, the parameter 'm' is still missing. To find the best value for this variable, we need to see the influence that the LED light has in the LDR, by changing it's values in a linear way, while calculating the illuminance read by the LDR. Doing this for different values of m, we can see the one that creates the most linear slope:

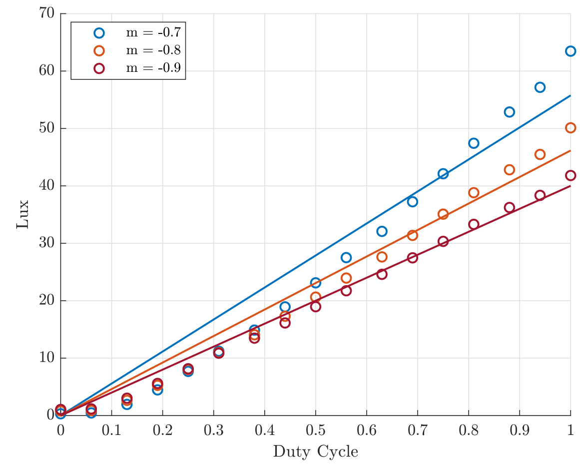

Fig. 5: Progression of LDR readings with Lux

The value of m = -0.9 creates the best coefficient of determination R^2 = 0.9952.

2) b parameter in PID: When computing $x(t_k)$ to get $u(t_k)$ (1), we multiply by the box gain G, so it can also be said that in order to do the backward computation, we can obtain $u_{ff}(t_k)$ by multiplying $r(t_k)$ by approximately G^{-1}, so when using the set-point transfer function:

$$\frac{X}{X_{ref}} = \frac{(bT_i s+1)(s\tau+1)}{(s\tau+1)\frac{T_i s}{GHK}+T_i s+1} \quad (14)$$

When calculating the steady state gain, equaling the transfer function to 1, we deduct that:

$$bKH \approx G^{-1} \quad (15)$$

To simplify the computation of b:

$$b = \frac{1}{GHK} \quad (16)$$

Where H is the value of $\frac{volt}{lux}$ of a certain reference. So when setting a fixed K, the b value computes it self after the system calibrates and every time the reference changes.

3) Ti parameter: From the set-point transfer function, it is deducted that Ti is approximately equal to the time constant τ. So, every time that the reference changes, it calculates the value of the theoretical τ:

$$\tau = R_{eq} * C \quad (17)$$

Where R_{eq} is the parallel between the LDR resistor and the $10k\Omega$ resistor, and C is the $10\mu F$ capacitor from 3.

$$T_i = \tau, \quad (18)$$

every time the reference changes. Although using the theoretical τ is not the perfect approach, it is a good approximation of the real value. The T_t parameter from the anti windup is always set to 0.1.

In Figure 6, the real values of τ are depicted as the light intensity changes across various duty cycles. Specifically, for a gain of nearly 35, the corresponding values of τ are:

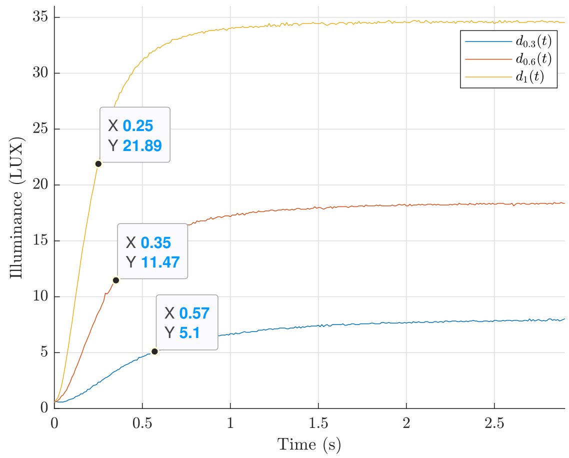

Fig. 6: Calculation of the real value of τ

- $dutycycle = 1 \leftrightarrow \tau = 0.25s$
- $dutycycle = 0.6 \leftrightarrow \tau = 0.35s$
- $dutycycle = 0.3 \leftrightarrow \tau = 0.57s$

When transporting the box, the Arduino units sometimes shift out of place, leading to collisions and altering the overall gain of the system. Consequently, recalibration of the values becomes necessary each time such incidents occur. To address this issue, I've decided to integrate the theoretical value for τ directly into the program.

This change ensures that even if the physical setup undergoes disturbances during transportation, the program maintains a consistent reference point, reducing the need for frequent recalibration.

A. Calculation of P_{max}

The energy consumption formula necessitates the knowledge of the maximum power dissipation at the LED. To determine this value, it is imperative to measure the current flowing through the 47Ω resistor. Subsequently, by calculating the current passing through the LED, we can accurately measure the voltage across the LED terminals. This comprehensive approach allows for the precise determination of power dissipation, contributing to an accurate assessment of energy consumption.

$$I = \frac{V_{resistor}}{R} \leftrightarrow I = \frac{0.29}{47}A \tag{19}$$

$$P_{max} = V_{LED}I \leftrightarrow P_{max} = 2.63 \cdot 6.17 \cdot 10^{-3} = 0.0162W \tag{20}$$

IV. Interface extras

Command	Request	Response
Set the value of b in luminaire i	'B i val'	'ack' or 'err'
Get the value of b in luminaire i	'g B i'	'B i val'
Set the value of K in luminaire i	'K i val'	'ack' or 'err'
Get the value of K in luminaire i	'g K i'	'K i val'
Set the value of T_i in luminaire i	'I i val'	'ack' or 'err'
Get the value of T_i in luminaire i	'g I i'	'I i val'
set the value of T_t in luminaire i	'T i val'	'ack' or 'err'
Get the value of T_t in luminaire i	'g T i'	'T i val'
Set bumpless transfer of desk i	'R i val'	'ack' or 'err'
get bumpless transfer of desk i	'g R i'	'R i val'
get gain of desk i	'g g i'	'g i val'

V. Results

A. Time response with different K values

The system was tested with different values of K, that as a consequence, influence the value of b with Equation 16.

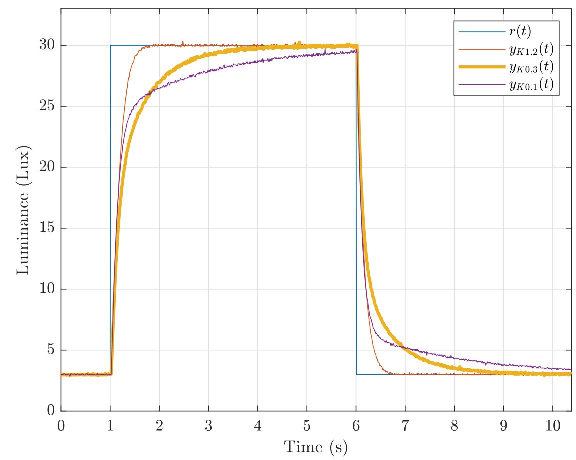

Fig. 7: Time response of the output with different K values

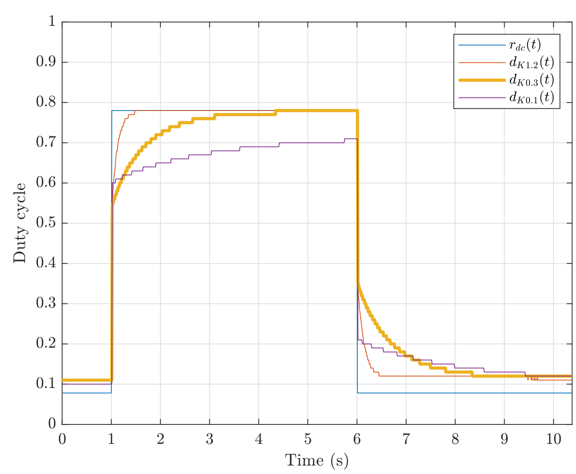

Fig. 8: Time response of the duty cycle with different K values

Observing Figure 7, it becomes evident that a lower value of $K = 0.1$ leads the proportional term to stabilize at an incorrect reference value. Due to the inherently slower nature of the integral term, it takes a considerable amount of time to eventually bring the system to the correct reference. On the other hand, with K=1.2, the system exhibits increased speed, but at the cost of having a very fast response to disturbances, which may not be conducive to user comfort.

Optimal performance appears to be achieved with K=0.3, as this value successfully addresses the shortcomings observed with other K values. The proportional term acts swiftly, facilitating a rapid stabilization of the duty cycle to the desired value without compromising system stability inducing discomfort to any user.

B. Time response to external light

In the initial experiment involving external light, both other luminaires were consistently set to emit maximum light, resulting in a sustained illumination level of approximately 15 Lux.

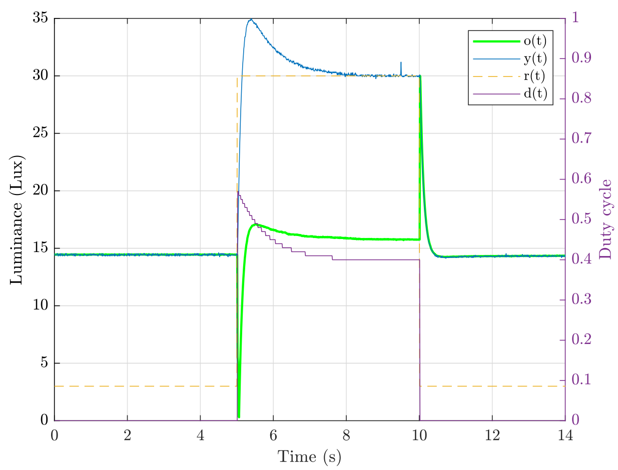

Fig. 9: Time response to a constant external light with pulsating reference

In Figure 9, when transitioning the reference value from 3 Lux to 30 Lux, a slight overshoot is observed in the system, attributed to the proportional term incorrectly perceiving the light level to still be at 3 Lux while in reality, it is around 15 Lux. However, this transient deviation is swiftly corrected by the integral term, which effectively stabilizes the system, aligning it with the correct reference value.

In the second experiment, the luminaire was maintained at a constant reference, while one of the other luminaires underwent pulsating light changes, alternating between its maximum value and being turned off.

In Figure 10, a discernible event unfolds around the 2-second mark, marked by the activation of the other luminaire. In response, the controller promptly adjusts its output, lowering its value to accommodate the influx of light from the newly activated source. Notably, at approximately 7.5 seconds, the luminaire is turned off once again, leading to a rapid and efficient convergence of the PID controller back to the reference value. This dynamic response underscores the system's agility in adapting to changes in the external

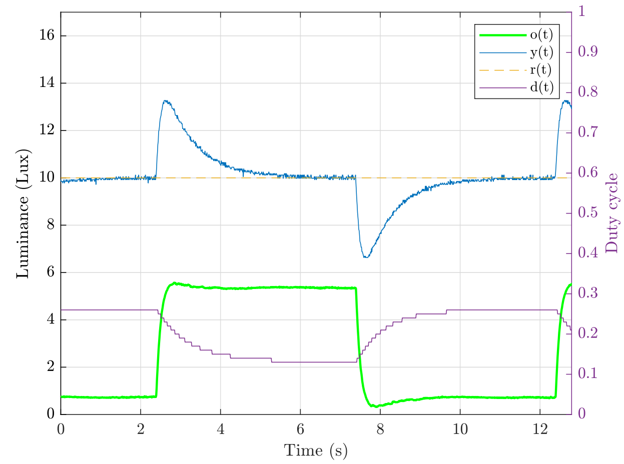

Fig. 10: Time response to a pulsating external light with constant reference

environment and swiftly restoring the desired illumination level.

C. Time response with and without anti windup

The objective of this experiment was to scrutinize the impact of the anti-windup enhancement in comparison to the standard PID control. For the initial 8 seconds, the system operated with the anti-windup feature activated. Subsequently, for the latter half of the experiment, the anti-windup was intentionally turned off. Concurrently, two additional luminaires were activated to establish a baseline level of illuminance within the system. This systematic manipulation allowed for a comprehensive analysis of how the absence of anti-windup influenced the performance of the PID control in the context of varying illuminance conditions.

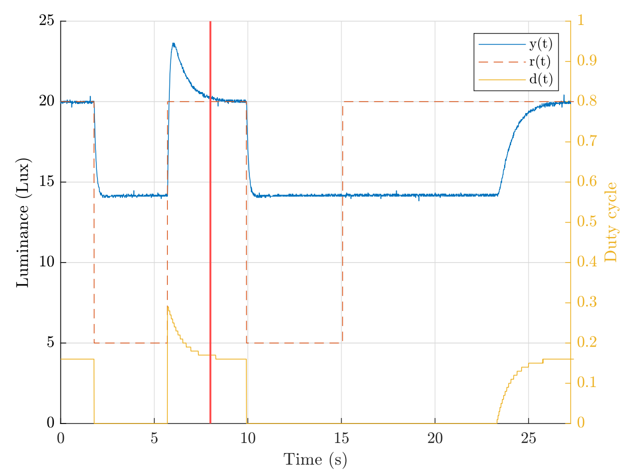

Fig. 11: Time response with anti windup

With the anti-windup feature enabled in Figure 11, a notable transition occurs around the 5-second mark, as the system shifts from the light being turned off (duty cycle = 0) to being activated. Despite the reference being set at 5 Lux, the presence of the other light being turned on prompts the system to automatically initiate convergence towards the reference value.

Conversely, when the anti-windup is deactivated, a distinct delay is observable around the 15-second mark following a change in the reference. During this period, the system takes approximately 9 seconds to recommence its efforts to converge to the new reference value. This delay is attributed to the integral term continually increasing the error while the system was saturated at a 0 duty cycle. Consequently, the prolonged accumulation of error requires additional time to rectify the event and resume convergence.

D. Time response with and without bumpless transfer

The experimental setup involves maintaining a constant reference while systematically varying the gain K within the range of 0.3 to 1 and subsequently returning it to the initial value of 0.3, as illustrated by the dashed lines in the plot. Notably, at the midpoint of the experiment, the bumpless transfer feature is deliberately deactivated. This strategic adjustment is designed to evaluate the system's response under changing K conditions, with a specific focus on the impact of bumpless transfer cessation during the latter part of the test.

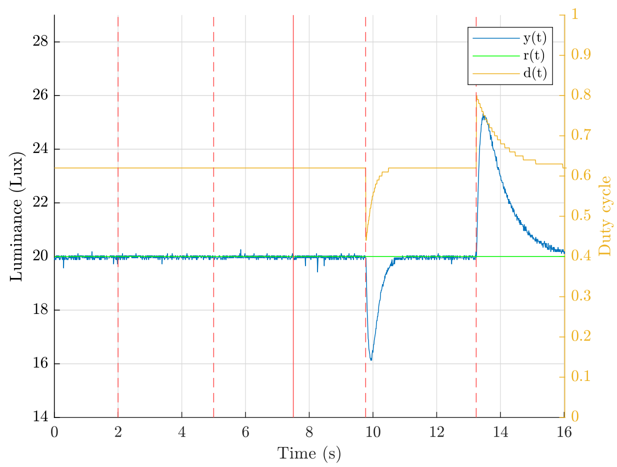

Fig. 12: Time response with bumpless transfer

In Figure 12, the efficacy of bumpless transfer activation is evident, showcasing the system's ability to seamlessly adapt to changes in the value of K. Notably, as K undergoes variation, the system adeptly responds to counteract these changes, ensuring a stable transition.

However, a pivotal moment occurs around the 7.5-second mark, marked by the deactivation of bumpless transfer. Consequently, the system loses its ability to effectively counteract the fluctuations in K, leading to a substantial and noticeable bump in the output $y(t)$. This abrupt deviation highlights the critical role of bumpless transfer in maintaining system stability during parameter changes.

E. Energy consumption

This experiment was conducted to assess the system's energy consumption, aiming to enhance its real-world performance evaluation. A low energy footprint is essential for the system's economic viability, while ensuring user comfort remains a priority. Around the 17-seconds mark, the feedback was turned of.

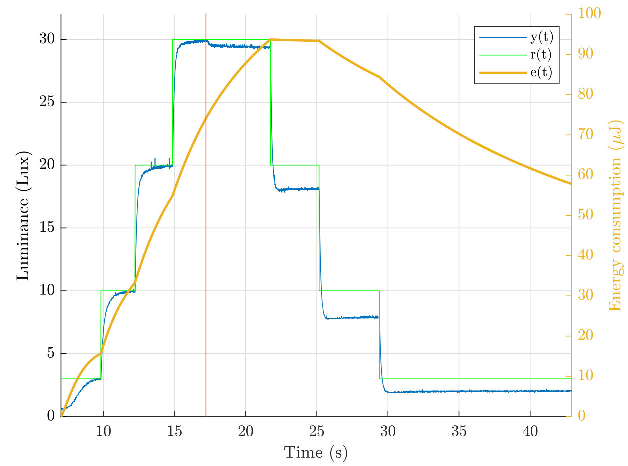

Fig. 13: Average energy consumption over time

Although not very noticeable, in Figure 13 when the system is at a higher illuminance (30 lux), the slope of the energy consumption is higher than when the illuminance is at around 10 lux, which is expected given to the fact that a higher light level requires a higher power output by the LED. If the test continued, the energy level would stabilize at a value indicating the energy consumption at that reference.

F. Visibility error

This test aimed to assess the visibility error over time, examining the variance between the reference illuminance and the readings captured by the LDR. The objective was to evaluate the system's accuracy in approximating values with the controller. Notably, around the 23-second mark, the feedback mechanism was temporarily disengaged for specific observations.

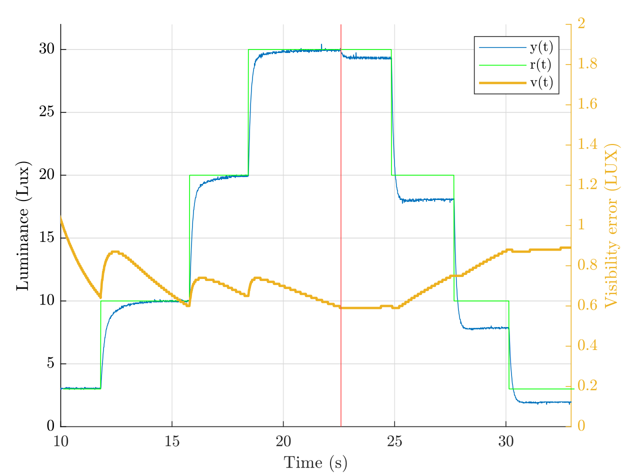

Fig. 14: Average visibility error over time

When the reference value undergoes a change, Figure 14, it is expected that the error will initially increase as the system adapts to accommodate the new value. However, this transient increase is swiftly followed by a subsequent decrease. Notably, when the feedback is turned off, the error stabilizes at a specific value, indicating the sustained difference in illuminance.

G. Flicker

In this experiment, a consistent reference value of 30 lux was maintained to observe the evolution of the flicker error over time. The experiment was conducted both with and without the implementation of the digital filter. This filter, positioned between controller measurements, captures 50 values from the LDR and computes their mean.

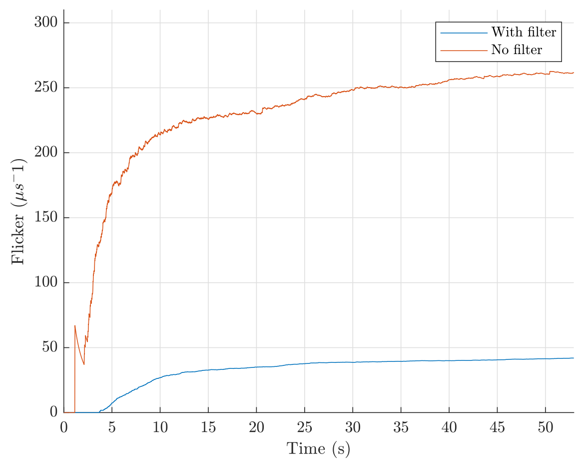

Fig. 15: Average flicker over time

As depicted in Figure 15, the implementation of the filter results in a relatively constant flicker error bellow 50 μs^{-1}. In contrast, without the filter, the flickering increases to around 250 μs^{-1} and continues to grow, highlighting the significant effectiveness of this filtering mechanism.

H. Jitter

The jitter is evaluated by computing the difference between the desired sample rate of 100Hz and the actual value of time between samples.

As illustrated in Figure 16, the sampling rate exhibits minimal deviation from the desired value, hovering around the microsecond range. However, there is a discernible trend indicating a gradual increase, primarily attributed to errors in the *Interrupt* function. Despite the controller's target sampling rate of 100Hz, the *Interrupt* implementation introduces small cumulative errors over time.

I. CAN-BUS communications

In this phase of the project, the communication between nodes is streamlined, requiring only the exchange of messages through a dedicated core and using *interrupts*. This setup allows for the simultaneous operation of the controller and the communication protocol, facilitating seamless coordination between the two processes with error checking at a maximum message sending rate of 15 ms without any errors from the can-bus.

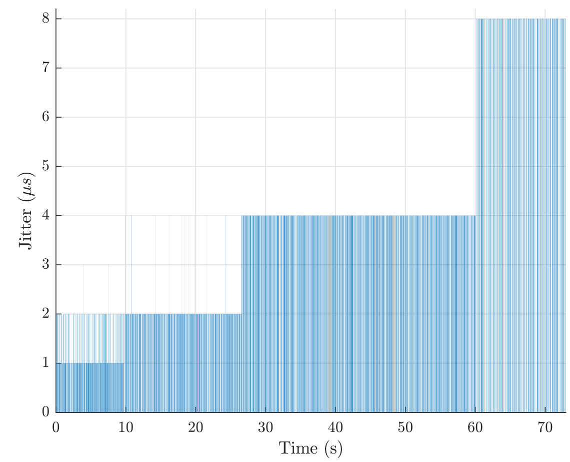

Fig. 16: Jitter over time

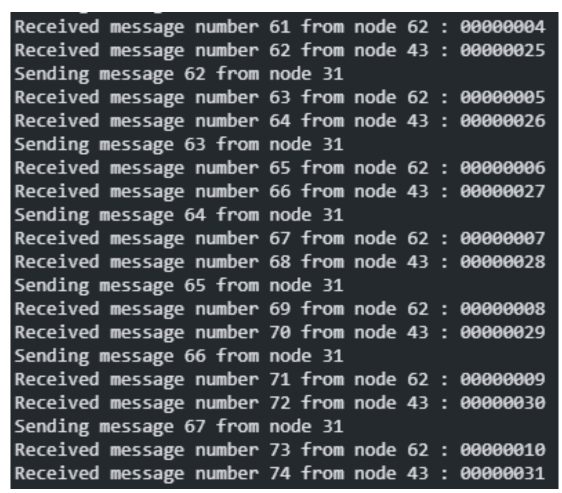

Fig. 17: Sending and receiving messages to and from all nodes

VI. Conclusions

This project has successfully addressed the challenge of designing and implementing a real-time illumination system utilizing a PID controller, Arduino Raspberry Pi Pico, and LDR sensor. Through a comprehensive methodology encompassing system modeling, parameter tuning, and experimental validation, significant insights have been gained into the efficacy and performance of the proposed system.

The utilization of a PID controller has proven instrumental in achieving smooth transitions between various light levels, ensuring optimal illumination in response to user preferences and external environmental changes. The incorporation of anti-windup and bumpless transfer mechanisms has further enhanced the system's stability and responsiveness, mitigating the effects of integral windup and facilitating seamless parameter adjustments during runtime.

Experimental results have provided valuable validation of the system's functionality and performance under diverse conditions, including changes in external light, parameter variations, and energy consumption considerations. Notably, the system has demonstrated rapid convergence to reference values, effective adaptation to external disturbances, and efficient energy utilization, highlighting its potential for real-world applications.

Furthermore, the implementation of additional features such as visibility error analysis, flicker reduction through digital filtering, and jitter assessment has underscored the system's robustness and reliability in achieving accurate and consistent illumination control.